Probiotics modulated gut microbiota suppresses hepatocellular carcinoma growth in mice

Jun Li[a,1], Cecilia Ying Ju Sung[b,1], Nikki Lee[c], Yueqiong Ni[a], Jussi Pihlajamäki[d,e], Gianni Panagiotou[a,2], and Hani El-Nezami[b,d,2]

[a]Systems Biology and Bioinformatics Group, School of Biological Sciences, Faculty of Sciences, The University of Hong Kong, Hong Kong S.A.R., China; [b]School of Biological Sciences, Faculty of Science, The University of Hong Kong, Hong Kong S.A.R., China; [c]Department of Surgery, Li Ka Shing Faculty of Medicine, The University of Hong Kong, Hong Kong S.A.R., China; [d]Insititute of Public Health and Clinical Nutrition, University of Eastern Finland, Kuopio 70211, Finland; and [e]Clinical Nutrition and Obesity Center, Kuopio University Hospital, Kuopio 70211, Finland

Edited by Sven Pettersson, Karolinska Institutet, Stockholm, Sweden, and accepted by the Editorial Board January 11, 2016 (received for review September 12, 2015)

The beneficial roles of probiotics in lowering the gastrointestinal inflammation and preventing colorectal cancer have been frequently demonstrated, but their immunomodulatory effects and mechanism in suppressing the growth of extraintestinal tumors remain unexplored. Here, we adopted a mouse model and metagenome sequencing to investigate the efficacy of probiotic feeding in controlling s.c. hepatocellular carcinoma (HCC) and the underlying mechanism suppressing the tumor progression. Our result demonstrated that Prohep, a novel probiotic mixture, slows down the tumor growth significantly and reduces the tumor size and weight by 40% compared with the control. From a mechanistic point of view the down-regulated IL-17 cytokine and its major producer Th17 cells, whose levels decreased drastically, played critical roles in tumor reduction upon probiotics feeding. Cell staining illustrated that the reduced Th17 cells in the tumor of the probiotic-treated group is mainly caused by the reduced frequency of migratory Th17 cells from the intestine and peripheral blood. In addition, shotgun-metagenome sequencing revealed the crosstalk between gut microbial metabolites and the HCC development. Probiotics shifted the gut microbial community toward certain beneficial bacteria, including *Prevotella* and *Oscillibacter*, that are known producers of antiinflammatory metabolites, which subsequently reduced the Th17 polarization and promoted the differentiation of antiinflammatory Treg/Tr1 cells in the gut. Overall, our study offers novel insights into the mechanism by which probiotic treatment modulates the microbiota and influences the regulation of the T-cell differentiation in the gut, which in turn alters the level of the proinflammatory cytokines in the extraintestinal tumor microenvironment.

hepatocellular carcinoma | probiotics | Th17 | IL-17 | metagenome

Hepatocellular carcinoma (HCC) is one of the most common cancers, the sixth most common neoplasm, and the second most deadly type of cancer worldwide (1). The traditional HCC treatment, including surgical treatment, local ablation therapy, and chemotherapy, could offer potential cure, yet patients are facing many limitations including the poor hepatic reserve. HCC is clearly a disease for which alternative therapeutic strategies must be developed. A better understanding of the interactions between cancer cells and stromal components in the tumor-associated proinflammatory microenvironment would be important for the management of this disease.

The tumor microenvironment is infiltrated with various immune cells such as T cells, macrophages, neutrophils, natural killer (NK) cells, and myeloid-derived suppressor cells. Inflammation is known to play a pivotal role in tumor development by escalating tumor angiogenesis and cell growth. Once a solid tumor is formed, inflammation arises in the tumor-promoting direction. At the same time, new vasculature is needed in the tumor to provide nutrients and oxygen to support the growth of cancer cells, and this process plays a critical role in HCC, a highly vascularized tumor (2). Inflammation and angiogenesis are closely linked processes and act to potentiate each other, supported by the dual functionality of proinflammation and proangiogenesis in many angiogenic factors, such as IL-17, IL-1β, and IFN-γ; therefore, modulating these two processes may exert a beneficial effect in controlling HCC growth (3).

T helper 17 (Th17) is a T-cell subpopulation, characterized by production of IL-17 cytokines, which can also be expressed by CD8+ T, macrophages, and neutrophils, etc. (4). The prevalence of Th17 cells was found to increase in the tumor microenvironment during tumor development (5). In addition, IL-17 plays a prominent role by increasing the angiogenic activity (6) via certain indirect mechanisms, such as (*i*) induction of IL-17–responsive cells to secrete proinflammatory cytokines, e.g., IL-6 and IL-1β, which also possess potent angiogenic activity (7); (*ii*) induction of a wide range of angiogenic mediators but inhibition of the angiostatic chemokine secretion (8); and (*iii*) induction of tumor and epithelial cells to secrete increasing levels of angiogenic chemokines (9). As mentioned above, HCC is a highly vascularized tumor; therefore, Th17/IL-17+ cells may play an important role in angiogenesis and progression of HCC.

The gut microbiota is the microbial population that resides in the gastrointestinal tract. It is now widely accepted that the whole

Significance

Hepatocellular carcinoma is the second most deadly cancer type globally, requiring the development of alternative or complementary therapeutic and prophylactic methods. Here, when feeding a mouse model with a novel probiotic mixture 1 wk before the tumor inoculation, we observed a reduction of the tumor weight and size by 40% compared with the control. Our results revealed that the probiotics' beneficial effect is closely related with the abundance of certain beneficial bacteria that produce antiinflammatory metabolites, which subsequently regulate the proinflammatory immune cell population via the crosstalk between gut and tumor. We believe that our study highlights the extraordinary potential of probiotics in extraintestine cancers and can be adapted to the study of other cancers.

Author contributions: N.L., G.P., and H.E.-N. designed research; J.L. and C.Y.J.S. performed research; J.L. and C.Y.J.S. analyzed data; J.L., C.Y.J.S., Y.N., and J.P. wrote the paper; and J.L., C.Y.J.S., and Y.N. visualized the data.

Conflict of interest statement: C.Y.J.S., N.L., and H.E.-N. are holders of a patent under the publication number US 2015/0164964A1, "Method and compositions for treating cancer using probiotics."

This article is a PNAS Direct Submission. S.P. is a guest editor invited by the Editorial Board.

Data deposition: The data reported in this paper have been deposited in the Sequence Read Archive (SRA) database, www.ncbi.nlm.nih.gov/sra (accession no. SRP062583).

[1]J.L. and C.Y.J.S. contributed equally to this work.

[2]To whom correspondence may be addressed. Email: gipa@hku.hk or elnezami@hku.hk.

This article contains supporting information online at www.pnas.org/lookup/suppl/doi:10.1073/pnas.1518189113/-/DCSupplemental.

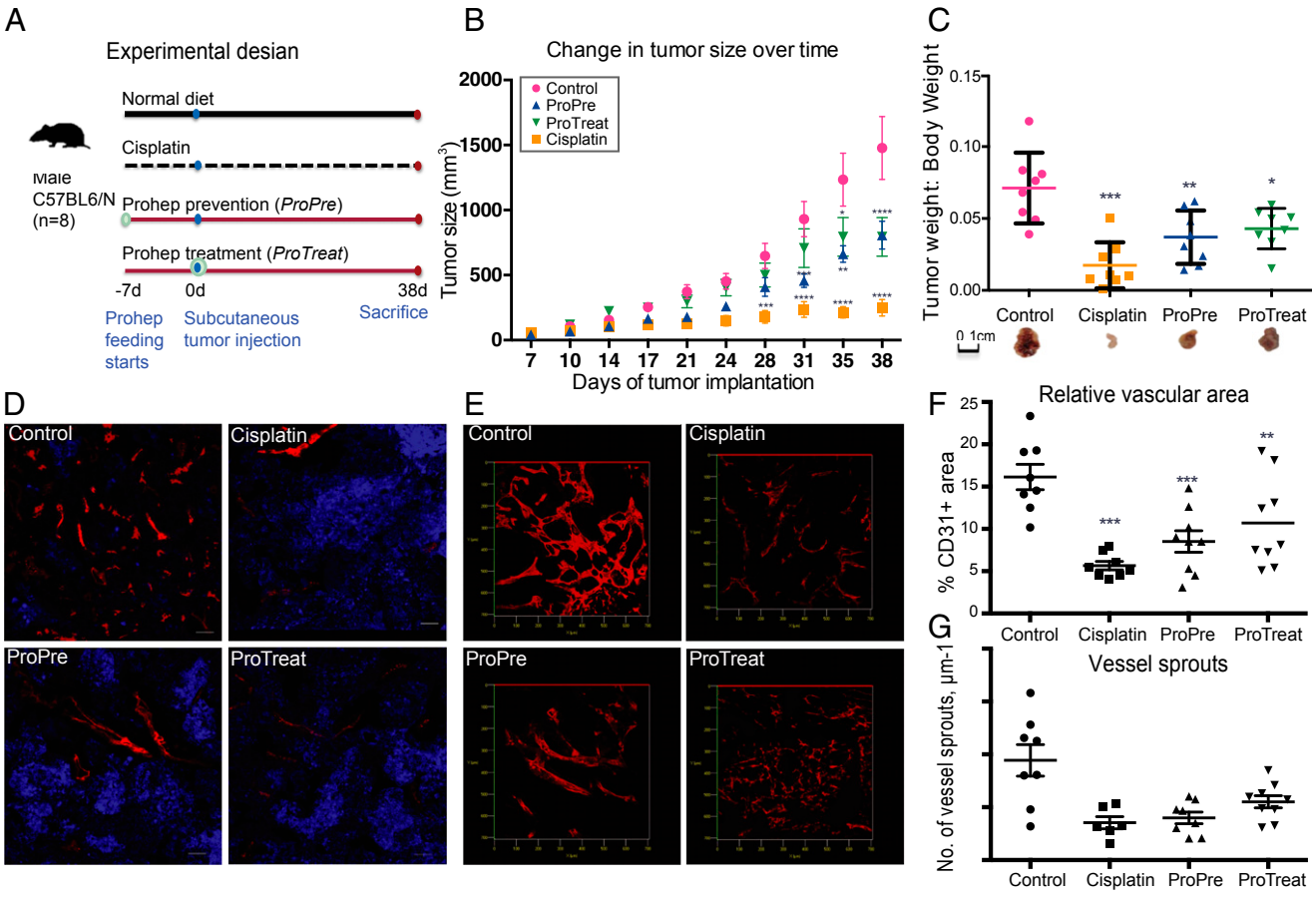

Fig. 1. Probiotics reduced the tumor size and increased hypoxia in the tumor. (*A*) Study design: Male 5–6 wk C57BL6/N mice ($n = 8$ in each group) were fed with Prohep daily starting 1 wk before or at the same day of s.c. injection of mouse hepatoma cell line Hepa1-6. Two extra groups, control (normal diet) and cisplatin, were also included for comparison. The animals were killed 38 d after tumor injection to quantify the tumor size. (*B*) Tumor size variation during 38 d of monitoring. (*C*) Distribution of tumor weight at the end of the experiment. (*D*) Immunostaining for representative tumor sections for the GLUT-1 (blue) hypoxic marker and CD31 (red) angiogenesis marker. (*E*) Images of 3D models obtained by confocal Z stacks, after superimposition of multiple confocal planes (section thickness, 25 μm). (*F*) Distribution of the relative vascular area in four groups at the end of experiments. (*G*) Distribution of vessel sprout in four groups at the end of the experiments. All of the statistical tests were performed using *t* test between each treatment group and control group. *0.01 < *P* value < 0.05; **0.001 < *P* value < 0.01; ***P value < 0.001.

community composition, in addition to some particular bacteria, influences the differentiation of the T-cell subpopulation in the intestine (10) and expansion in the lamina propria (11). In relation to cancer it is known that some infectious agents, including *Helicobacter pylori* as well as hepatitis B and C viruses, contribute to carcinogenesis (12). It has also been shown that the intake of probiotics, health-beneficial bacteria, exhibited an antiinflammatory effect by inducing Tregs in gut and alleviated the severity of some inflammatory diseases through suppressing the Th17 differentiation (13). Although, at the molecular level, the mechanisms of action of probiotics are largely unknown, probiotics can act at least with the following mechanisms: (*i*) modulate the gut microbiota and suppress the growth of pathogenic microorganisms; and (*ii*) interact with the mucosal system, which affects the systemic immunity.

In this study, we evaluated the efficacy of a novel probiotic mixture (Prohep) (see *SI Methods* and Fig. S1 for detailed description) on hepatocellular tumor growth in mice and the relationships between tumor suppression, angiogenesis, and modulation of Th17 cells and IL-17. We further applied whole genome shotgun metagenome sequencing to develop a molecular roadmap of the interactions between the probiotic-modulated gut microbiota and their metabolic products with the T-cell differentiation, secretion of antiinflammatory cytokines, and HCC tumorigenesis.

Results

Probiotics Reduce the Liver Tumor Growth by Inhibiting Angiogenesis. To determine whether probiotics could exhibit therapeutic potential, the probiotic mix Prohep was administered orally on a daily basis starting from either 1 wk in advance (*ProPre*) or at the same day (*ProTreat*) of tumor inoculation. Two extra groups, control and cisplatin, were also included to compare the therapeutic efficacy (Fig. 1*A*). During the 38 d of tumor monitoring, we observed that s.c. HCC growth was effectively reduced in the Prohep-treated groups. The average tumor volume in the *ProTreat* group was significantly smaller (40%) than that in the control group from day 35; however, when Prohep was administered 1 wk before the tumor inoculation (*ProPre* group) the beneficial effect could be observed even earlier (from day 31) (Fig. 1*B*). Even though cisplatin has elicited its anticancer effect already from day 28 (earlier than *ProPre* and *ProTreat*), the difference of tumor weight/body weight between *ProPre* and cisplatin was statistically insignificant at the end of the experiment (day 38) (Fig. 1*C*). We also found that, at the end of experiment, the tumor weight in the *ProPre* group was significantly smaller (41%, on average) than in the *ProTreat* group (Fig. 1*C*), revealing that early feeding of probiotic preparations could lead to better antitumor effects.

Because the tumor growth may be inhibited through several processes, such as decreased cell proliferation, increased cell

death, or increased hypoxia, we used immunohistochemistry staining of the tumor tissue (38 d) to identify the direct causes of tumor suppression in the Prohep (*ProPre* and *ProTreat*) and cisplatin groups. The result revealed no significant difference in the number of proliferative (Ki67+) cells or apoptotic (caspase-3+) cells (Fig. S2) between the control and Prohep groups, suggesting that the smaller tumor sizes in the probiotic groups are unrelated with reduced proliferative tumor cells or enhanced apoptosis in tumor. We further evaluated the hypoxic regions in the 38-d tumor sections in all groups using hypoxic (GLUT-1+) marker staining. The result revealed a significant increase (47%, on average) in the hypoxic (GLUT-1+) area in the *ProPre* group, suggesting that the reduced tumor size was likely to correlate with hypoxia-induced cell death (Fig. 1*D* and Fig. S3). Although low glucose level could also induce a high level of GLUT-1, hypoxia would be the most possible cause of the increased GLUT-1 in our study due to the following reasons: GLUT-2, instead of GLUT-1, mediates glucose uptake in hepatocyte (14); therefore, a low glucose level in liver cancer cells may not trigger the overexpression of GLUT1; there is a documented strong association between hypoxia and liver tumor (15, 16) that correlated the increased hypoxia with the observation of high level of the GLUT-1 in our study.

To test whether the increased hypoxia of tumor cells in the Prohep groups was related to the weakened angiogenesis, we used 3D models by confocal Z stacks to evaluate the microvessel density (MVD), relative vessel vascular area, and number of vessel sprouts. As shown in Fig. 1 *E*–*G*, the MVD, the percentage area of blood vessel per tumor section, and the number of vessel sprouts were all significantly lower (52% and 54% for blood vessel area and vessel sprouts, respectively) in the Prohep groups than those in the control group, suggesting that Prohep treatment might limit tumor growth by reducing angiogenesis, and so forth lead to hypoxia-induced cell death in tumor.

Probiotics Down-Regulate *IL-17* and Other Proangiogenic Genes in Liver Tumor. To investigate the potential causes of the reduced angiogenesis in tumor by probiotics, we evaluated the expression level of 62 genes associated with angiogenesis or immunoregulation in the 38-d tumor sections from 32 mice (each treatment group contains 8 mice). We found that many important angiogenic growth factors and receptors, including FLT-1, *ANG2*, *KDR*, *VEGFA*, and *TEK*, were down-regulated (range from 52 to 81%) in the Prohep groups compared with the control (Fig. 2*A*). At the same time, the expression level of the adhesion molecule *VE-cadherin* and some common growth factors such as *TGF-β* were also reduced (by 65% on average) in the Prohep groups (Fig. 2*A*). The Th17 marker genes, *IL-17* and RORγt, were reduced in the Prohep groups by 65% and 85%, respectively, compared with the control group. We also observed that the expression level of two antiinflammatory cytokines IL-27 and *IL-13* increased exclusively in the Prohep feeding groups but not in the cisplatin group (Fig. S4 *A* and *B*). Furthermore, there was significant increase of antiinflammatory cytokine IL-10 in the *ProPre* group by 102% and in the *ProTreat* group by 98%, compared with the control (Fig. 2*A*). This result revealed that the reduced tumor size by the probiotics treatment is strongly associated with the decreased expression of proangiogenic genes. In addition, we noticed a higher expression of the hypoxia-inducible factor 1 (*HIF-1*) in the *ProPre* group than in the control group. Because *HIF-1* could induce high level of *GLUT-1* under hypoxia conditions (17), the aforementioned higher level of *GLUT-1* (Fig. 1*D*) in the *ProPre* group suggested an increased hypoxia in this group.

We further carried out correspondence analysis to investigate the common patterns of the expression profiles among the 62 genes in different groups. The result showed that the two Prohep groups (*ProPre* and *ProTreat*) are sharing similar expression profiles (similar coordination), whereas the cisplatin group is distantly positioned compared with all other groups, implicating the different mechanism of tumor size reduction between the probiotics and anticancer drug (Fig. 2*B*). As shown in Fig. 2*B*, one cluster of genes (hierarchical clustering based on Euclidian distance) was composed of many angiogenic markers including FLT-1, *ANG2*, *KDR*, and *VEGFA*, as well as the adhesion molecule *VE-cadherin* and common growth factors such as *TGF-β*. The expression levels of the genes in this group were down-regulated in the Prohep treatment groups (Fig. 2*A*). The expression level for most of these genes was also decreased in the cisplatin group, indicating some common effects of the probiotic feeding and anticancer drug in the tumor microenvironment. The second group of genes, containing *TEK* and Th1-cell-released angiogenesis factors *IL-17A*, *IFNG*, *IP10*, *STAT4*, and *TBET*, were down-regulated in the Prohep groups but up-regulated in the cisplatin group (Fig. 2*B* and Fig. S4 *C*–*F*), revealing the exclusive association between reduced tumor size and other proinflammation T cells in the Prohep treatment group.

Because our results revealed the down-regulation of the *IL-17* expression in the Prohep groups, we investigated next whether the reduced tumor growth by probiotics intake is strongly associated with *IL-17* modulation. We injected mice with *IL-17* antibodies 1 wk before tumor inoculation, and the tumor size was monitored for 1 mo. The *ProPre* study design was used due to its better efficacy in reducing the tumor growth. Animals with anti–*IL-17* and control diet have shown significantly smaller tumor volume and weight compared with mice (*i*) with control diet and without anti–*IL-17* and (*ii*) with Prohep intake and without anti–*IL-17* (Fig. 2*C*), suggesting the adverse effects that *IL-17* exerted on tumor development. In addition, Prohep presented antitumor effect in mice without anti–*IL-17* treatment, whereas it failed to further reduce the tumor size after *IL-17* neutralization by comparing two groups with *IL-17* antibodies (Fig. 2*C*). The results from this IL-17 inhibition experiment imply that Prohep may require *IL-17* modulation to suppress the tumor growth. It should be noted here that an alternative explanation for this observation could be that the anti–*IL-17* has much stronger anticancer effect than the Prohep intake by suppressing the inflammation and angiogenesis in tumor. Further analysis revealed that, in addition to the tumor size, the reduced angiogenesis (MVD) in Prohep groups is also dependent on the *IL-17* (Fig. S5).

Probiotics Affect Th17 Distribution and Mediate Th17 Polarization. The aforementioned results revealed an association between reduced tumor growth and the decreased IL-17 secretion in the tumor. Because various cell types, including T cells, macrophage, and neutrophils, are capable of secreting IL-17, we used immunostaining of IL-17 together with several immune cell surface markers to identify the primary IL-17 producing cell subsets modulated by the Prohep feeding. We found that in all experimental groups the majority of IL-17+ cells in the tumor were CD3+ cells, whereas only a small portion was macrophages (Fig. 2 *D* and *E*). In addition, there is no significant difference regarding the proportion of IL-17+ cells costained with CD3+ between the four treatment groups (Fig. 2*E*). Because CD3+ cells are composed of CD+4 T cell, CD8+ T cell, and NK cell subpopulations, and all these subpopulations are known to express IL-17, we further used flow cytometry to reveal whether certain CD3+ subpopulations differ among the treatment and control groups. As shown in Fig. 2*F*, there was slightly reduced infiltration of CD4+ T cells in the *ProPre* and cisplatin groups. We further compared the IL-17 production in different CD3+ subpopulations and found that IL-17 expression was restricted to CD4+ cells in the tumor sections with no significant difference between groups (Fig. 2*G*).

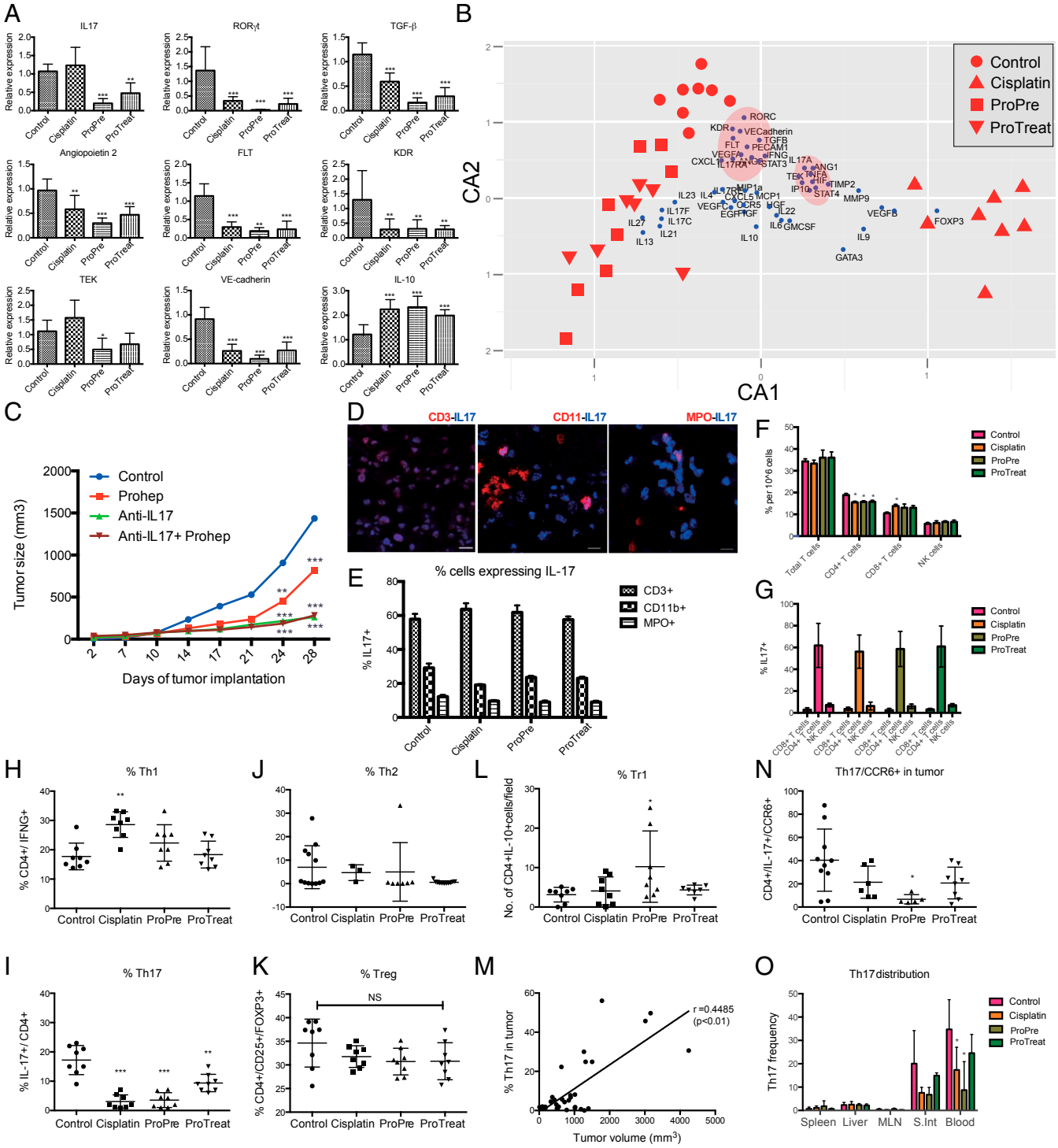

Fig. 2. Probiotics retarded the tumor growth and its association with Th17 and IL-17. (*A*) Down-regulated IL-17 and other angiogenic factors, and up-regulated IL-10 in the two Prohep groups in 38-d samples. (*B*) Correspondence analysis of the qRT-PCR results of 38-d samples in four groups. (*C*) Tumor size variation during 38 d of monitoring with anti-IL-17 antibody. (*D*) Confocal images of tumor sections with IL-17 staining (blue), costained (red) with CD3 T cells (*Left*), CD11b macrophage (*Center*), and MPO neutrophils (*Right*). (*E*) Percentage of cell expressing IL-17 in CD3+, CD11b+ and MPO+ cells. (*F*) Frequency distribution of subpopulation of CD3+ cells in three groups. (*G*) Distribution of IL-17 production among different cell types. (*H–L*) Frequency of subpopulation of T cells in tumor: Th1 (*H*), TH17 (*I*), Th2 (*J*), Treg (*K*), and Tr1 (*L*). (*M*) Positive correlation between the Th17 proportion and tumor volume. (*N*) Frequency of migratory Th17 cells in the tumor section. (*O*) Th17 frequency in various organs measured by flowcytometry. All of the statistical tests were performed using *t* test between each treatment group and control group. *0.01 < *P* value < 0.05; **0.001 < *P* value < 0.01; ***P value < 0.001.

To reveal which subpopulation of CD4+ cells could be modulated in the tumor by Prohep feeding, we used immunostaining and flow cytometry to investigate frequency distribution in Th1, Th2, Th17, Treg, and Tr1 in the four treatment groups. As shown in Fig. 2 *H–K*, there was no significant difference in Th1, Th2, and Treg subsets among all groups; however, the Tr1 frequency

is significantly higher in the *ProPre* group than that in other groups (89%, on average) (Fig. 2*L*). Considering that two extreme large values in the *ProPre* group (Fig. 2*L*) could possibly lead to an overestimated increase of Tr1, we excluded these two highest values in the *ProPre* group and performed the statistical test again. The result shows that the Tr1 frequency in *ProPre* group was still significantly higher than in the control group (Fig. S6). We also found that the population of the Th17 subset was significantly reduced within tumor in both Prohep groups (*ProPre* and *ProTreat*) compared with the control group (Fig. 2*I*). In depth analysis revealed that there is significant positive correlation ($R = 0.45$ and P value < 0.01) between the tumor volume and the Th17 frequency (Fig. 2*M*) in all of the groups. Our findings provide evidence that the retarded HCC development in the Prohep groups was associated with the increased antiinflammatory Tr1 cells, as well as the reduced population of proinflammatory and proangiogenic Th17 cells, which have been identified as the major producer of IL-17 in tumor. Although the overall decrease of the CD4+ in the Prohep groups compared with the control group is relatively small (3%), the reduction of the Th17 subpopulation in the Prohep groups is more drastic (~10% of CD4+), suggesting that the subpopulation of CD4+ played a more critical role in reducing the tumor size than the whole CD4+ cells. Interestingly, we also noticed that the proinflammatory Th1 cells are significantly increased in the cisplatin group, which partially explained the overexpressed angiogenesis factors in our quantitative PCR (qPCR) result.

Furthermore, to determine whether the lowered Th17 population within the tumor in the probiotics groups was caused by reduced Th17 cells recruitment, we quantified the expression of the chemokine receptor CCR6 (migratory phenotype) on Th17 cells in the tumor. We observed that the percentage of Th17 cells expressing this chemokine receptor was, on average, 64% lower in the *ProPre* group than that in the *ProTreat*, cisplatin, and control, respectively (Fig. 2*N*), which suggested that the preventive probiotic feeding might reduce the recruitment of Th17 cells to the tumor. Although there was a decreased number of CCR6+Th17 cells in the *ProTreat* group compared with the control group, the difference is not significant, illustrating that immunomodulation by Prohep in advance has much higher beneficial effect in reducing the tumor growth. Due to the reduced migratory phenotype in Th17 cells in the tumor of Prohep treated samples, we further investigated which periphery site these cells were recruited from. We quantified the distribution of Th17 in various organs, including spleen, liver, peripheral blood, mesenteric lymph node (MLN), and small intestine (shown in Fig. 2*O*). The proportion of Th17 cells in total CD4+ cells, was no different in spleen, liver, MLN among all four groups. However, the Th17 frequency (proportion of Th17 in CD4+ cells) was significantly reduced by 66% and 26% in peripheral blood in the *ProPre* and *ProTreat* groups, compared with the control group (Fig. 2*O*). A similar pattern of reduced Th17 frequency was observed in the small intestine (45% and 16% for *ProPre* and *ProTreat*, respectively) (Fig. 2*O*), suggesting that Th17 cells associated with the reduced tumor size were influenced by the decreased recruitment from the intestine to the tumor via the cardiovascular system. Collectively, Prohep feeding may reduce the Th17 frequency in intestine, and thus reduce the recruited Th17 in the tumor microenvironment. The reduced Th17 cells in the tumor could impede the inflammation and angiogenesis and limit the tumor growth.

Probiotics Mediate the Structural and Functional Composition of Gut Microbiota. Because previous studies revealed the close relationship between the composition of gut microbiota and metabolic diseases, inflammation, or colon cancer (18, 19), we further investigated how gut microbiota have changed upon Prohep feeding during the HCC development. The taxonomy profiles at the genus level revealed that the gut bacteria community in the mice was dominated by Bacteroidetes (49% on average), Firmicutes (37% on average), and Proteobacteria (4.5% on average) (Fig. S6). During the tumor progression, the relative abundance of Bacteroidetes increased more drastically in *ProPre* (fold change: 2.1) and *ProTreat* (fold change: 1.6) groups than in the control (fold change: 1.4) and cisplatin (fold change: 1.4) groups. Because previous studies revealed that bacteria from the phylum of Bacteroidetes could efficiently ferment fiber into acetates and propionates (20), the highly escalated Bacteroidetes levels in the Prohep-treated groups suggests a higher capability of producing acetate and propionate in the gut. In contrast, Firmicutes and Proteobacteria decreased (48–26% and 6.2–3.8% for Firmicutes and Proteobacteria, respectively) in all groups (Fig. S7). This consensus shift toward the increased Bacteroidetes and decreased Firmicutes among all groups revealed how the tumor progression and other common environmental factors influenced the gut microbiota. The hierarchical clustering result based on the relative abundance of different phyla shows that baseline samples have very similar community composition among four groups, whereas the four 38-d samples share more similar community structure (Fig. S7). The 38-d probiotic treatment sample (*ProTreat*D38) displayed a closer community composition compared with the 38-d preventive probiotics sample (*ProPre*D38), whereas the 38-d cisplatin treated sample (CisplatinD38) shows a distant relationship with all three samples at the same time point, serving as the outgroup in the cluster, suggesting the distinct influence of Prohep and cisplatin in shaping the gut microbiota.

When comparing the taxonomy profile of the four groups at the genus level, we found that with the exception of *Mucispirillum*, the relative abundance of other major genera (>1% relative abundance in at least one sample) in the Proteobacteria phylum decreased in all samples at the 38th day (Fig. 3*A*). Furthermore, the relative abundance of most (8 of 11) of the major genera in Firmicutes decreased, whereas about >55% (5 out of 9) of the major genera in Bacteroidetes increased the relative abundance in all four groups after 38 d. This consensus of the variation pattern of the genera abundance reveals that the common factor (e.g., tumor progression) in all four groups was the major driver of the gut community composition. However, some genera, e.g., *Alistipes* and *Oscillibacte*, showed distinct patterns regarding the variation of the relative abundance among different treatment groups. We next examined the taxonomic alpha diversity (Simpson diversity) within each sample. As shown in Fig. 3*B*, *Upper*, the alpha diversity decreased drastically (50% on average) in all groups after 38 d. This loss of community diversity can be explained by the tumor-induced dysbiosis in the gut bacteria community, consistent with previous findings that some diseases could lead to an imbalanced gut microbiota and decrease the ecological diversity in the gut (21, 22). When comparing the alpha diversity between the 38-d samples, we observed no significant difference between the control and *ProTreat* groups; however, cisplatin and *ProPre* groups showed significantly higher alpha diversity than both the control and *ProTreat* (Bonferroni adjusted P value < 0.05, Wilcoxon rank-sum test using 100 bootstrap samples). The *ProPre* presented the highest alpha diversity from all groups in the 38th day, suggesting that the preventive probiotics intake has the highest efficacy in rebalancing the gut microbiota to a healthy status.

To examine the shift of the community structure in terms of taxonomic and functional composition, we calculated both the taxonomic beta diversity (weighted Unifrac distance) and functional beta diversity (Bray–Curtis dissimilarity) between the groups. As shown in Fig. 3*B* the *ProPre* and cisplatin groups drastically shifted the community in both taxonomic and functional perspective, suggesting that the preventive Prohep and cisplatin treatment have the strongest effect in reshaping the community structure. The pattern of the drastic shift of gut

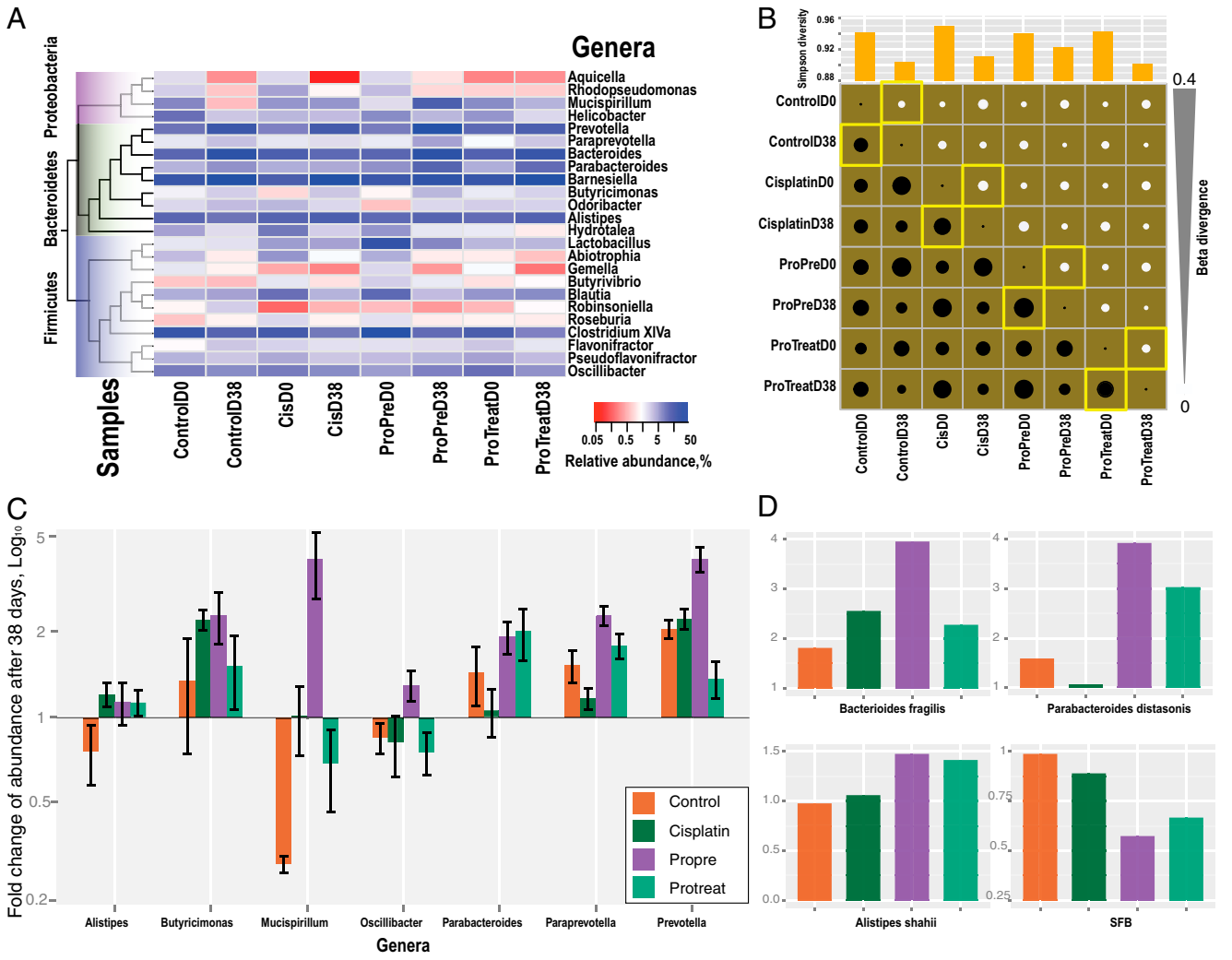

Fig. 3. The effect of probiotics feeding on the composition and diversity of gut microbiota. (*A*) Taxonomy distribution at genus level in different samples. (*Left*) The phylogenetic relationships and the affiliated phylum for each genus. (*B*) Simpson diversity (*Upper*), pairwised Unifrac distance (*Lower Triangle*), and Bray-Curtis dissimilarity (*Upper Triangle*) between samples. The yellow square frame highlighted the within group beta-diversity. (*C*) Significantly enriched genera in the *ProPre* group. The fold change (38-d vs. baseline) of these genera in all four groups were displayed. (*D*) Significantly enriched or depleted species in the *ProPre* group.

microbial composition in *ProPre* and cisplatin coincides with what we observed in the experiments of tumor size reduction (these two groups were the most efficient). In addition, the 38-d cisplatin sample displays a more distant relationship with the other 38-d samples considering the pairwised taxonomic beta diversity (Fig. S8), suggesting that the anticancer drug treatment affected the community structure in a different way compared with the probiotics. This diverged relationship between the 38-d drug sample and other samples is consistent with the aforementioned qRT-PCR results, where the probiotics intake and cisplatin treatment were associated with different expression profiles of genes related to angiogenesis or immunoregulation.

Probiotic Increase the Antiinflammatory Bacteria and Metabolites in Intestine. To address whether Prohep intake has the capability of inhibiting tumor progression through modulating the gut microbiota, we identified all of the significantly enriched genera (38-d vs. baseline) in the *ProPre* group. As shown in Fig. 3*C*, there are seven significantly enriched (Bonferroni adjusted P value $<$ 0.05 in Wilcoxon rank-sum test using 100 bootstraps for each sample) major genera: *Alistipes*, *Butyricimonas*, *Mucispirillum*, *Oscillibacter*, *Parabacteroides*, *Paraprevotella*, and *Prevotella*. Three of these enriched genera are related with short-chain fatty acids (SCFAs) production. *Butyricimonas*, a butyrate producer (23), and *Prevotella*, a propionate producer (24), increased the relative abundance more dramatically in the *ProPre* group than in the other groups. The relative abundance of *Alistipes*, a major SCFAs producer in gut (25), decreased in the control group but increased in the *ProPre* and *ProTreat* groups by 32% and 29%, respectively. Among other enriched genera in the *ProPre* group, *Oscillibacter* and *Parabacteroides* are associated with T-cell differentiation by enhancing and maintaining the IL-10 producing Treg cells (26, 27). One major species of the genus *Parabacteroides*, *Parabacteroides distasonis*, has the ability to reduce the intestinal inflammation by inducing the antiinflammatory cytokine IL-10 and suppressing the secretion of inflammatory cytokine IL-17, IL-6, and IFN-γ (26). *Oscillibacter* is a valerate producer and capable of enhancing the differentiation of IL-10 producing Tregs in vivo (27). Besides the enriched genera, we further identified five significantly enriched species (relative abundance > 0.1%) in the *ProPre* group, namely *Bacteroides fragilis*, *Alistipes shahii*, *Parabacteroides distasonis*, and *Akkermansia muciniphila*. *B. fragilis* is

well known for its immunoregulatory role in the gut by intriguing IL-10 producing Treg cells (28). Although the relative abundance of *B. fragilis* also increased in the control group, the fold change of the abundance is much higher in the *ProPre* group than in the control (3.8 vs. 1.7) (Fig. 3*D*). One recent study revealed the important role of *A. shahii* in the gut as a modulator in the suppression of tumor growth (29), and our findings showed an increase of this species in *ProPre* (48%) and *ProTreat* (39%), but remain unchanged in control and cisplatin groups. In addition, our result shows a much higher increase of the *P. distasonis* in *ProPre* and *ProTreat* than in control and cisplatin groups (Fig. 3*D*), suggesting that the intestinal inflammation could be attenuated in the Prohep groups due to the antiinflammatory characteristics of this species (26). Besides the significantly increased species, we also noticed that the major Th17-inducing bacteria, segmented filamentous bacteria (SFB), decreased dramatically in the *ProPre* and *ProTreat* groups but remained at a similar level in the control group, suggesting that the proinflammation activities from particular pathogens in the intestine were also suppressed upon probiotics feeding. In summary, the shifted gut microbiota in Prohep-treated groups is toward an increased abundance of many beneficially antiinflammatory bacteria, as well as decreasing the Th17-inducing bacteria.

In addition to the enriched taxonomic units, we also identified 97 enriched MetaCyc pathways or pathway classes in the *ProPre* group by comparing the enzyme abundances in each pathway (38-d vs. baseline). As shown in Fig. 4*A*, the overall enriched pathway classes (MetaCyc class I and II) are related to TCA cycle, fatty acids, and lipid biosynthesis, glycolysis, fermentation, carbohydrates, and carboxylate degradation. Closer inspection revealed that within "TCA cycle," "carboxylates degradation," and "fermentation" classes, many enriched pathways are associated with short-chain fatty acids (mainly acetate and propionate). Among the top 15 significantly enriched pathways in the *ProPre* groups, around one-third of them are correlated with the production of acetate ("acetate formation from acetyl-CoA I," "lysine fermentation to acetate and butyrate," "TCA cycle VII"), pyruvate ("Entner–Duodoroff Pathways"), or propionate ("conversion of succinate to propionate," "pyruvate fermentation to propionate I") (Fig. 4 *B* and *C*). Several significantly enriched pathways in Prohep have also been enriched in control group, but the fold change in these pathways is much smaller than that in the *ProPre* group. Only the pathway of "conversion of succinate to propionate" was enriched in the cisplatin group, again indicating the distinct mechanism of tumor suppression between probiotics intake and normal anticancer drug treatment. This drastically increased metabolic potential in SCFAs (acetate and propionate) producing is concordant with our taxonomy analysis because the increased phylum Bacteroidetes and most of the enriched genera are related to SCFAs production.

Besides the enhanced SCFAs producing pathways, the biogenesis of certain compounds may also relate to the enhanced antiinflammatory activities of the *ProPre* group in the top 15 enriched pathways. Our enrichment analysis indicates that two long-chain fatty acids, palmitoleate and docosahexaenoate (DHA), enhanced their biogenesis potential in the *ProPre* group (Fig. 4*B*). Palmitoleate has been documented to exert antiinflammation effect in mice by down-regulating the proinflammatory cytokines

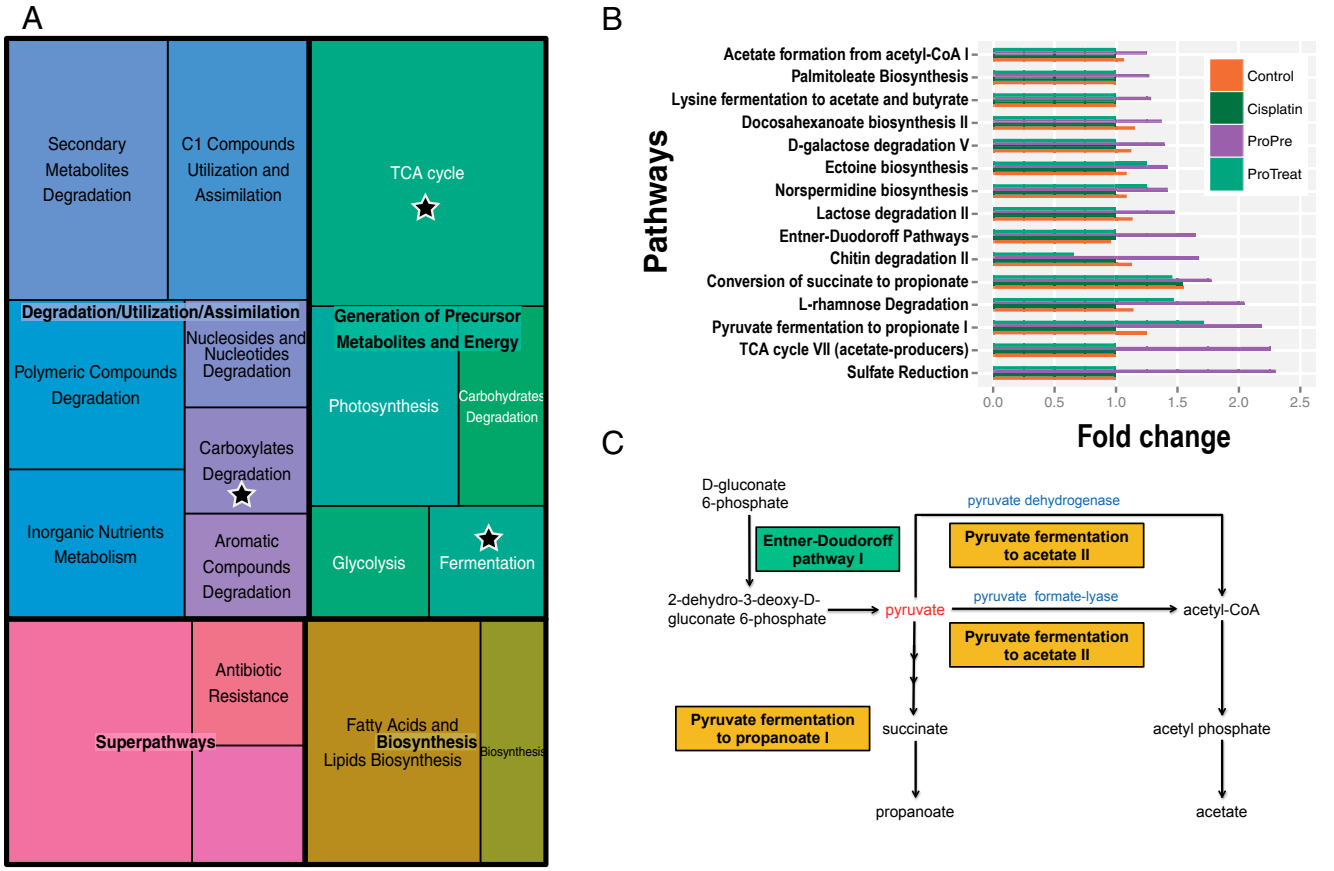

Fig. 4. Significantly enriched pathways in the *ProPre* group. (*A*) Significantly enriched MetaCyc pathways classes (I and II). The stars highlighted the pathways related to SCFAs synthesis. (*B*) Top-15 significantly enriched pathways; If no significant difference was detected between the tested and control group, the fold-change would be set to 1. (*C*) Enriched pathways related to pyruvate fermentation and SCFAs.

(30), whereas the omega-3 fatty acid docosahexaenoate can reduce the proinflammation cytokines in endothelial cells (31). Putting the pieces together, the metagenome analysis revealed that the functional shift of the gut microbiota in the preventive Prohep treated group was toward a more antiinflammatory metabolic environment, which could suppress the secretion of Th17 cells in the gut and subsequently reduce the recruitment of Th17 to liver, consistent with our experimental results.

Discussion

Our results offer novel insights into the mechanism by which probiotics modulate the microbiota and influence T-cell differentiation in the gut, which influences the differentiation of pro- or antiinflammatory cytokines in the HCC microenvironment. This study highlights the therapeutic potential of probiotics in HCC treatment and their global influences in extraintestine sites. In the past decades, many antiangiogenic agents such as sorafenib (32) have been adopted for HCC treatment. However, most of the patients with advanced-stage HCC do not benefit from these therapies due to its transient survival benefits (32). Meanwhile, other antiangiogenic therapies such as transcatheter arterial chemoembolization (TACE) typically face with aggressive tumor regrowth due to exacerbation of tumor hypoxia, increased vascular endothelial growth factors (VEGF) expression, and inflammation. In this study, mice receiving cisplatin treatment reduced the food intake and lost weight more drastically than other groups (Fig. S9), suggesting the importance of alternative therapeutic methods.

Our study revealed that the novel probiotic mix Prohep was effective to reduce s.c. HCC growth in mice by almost 40% especially when the probiotics were administrated before the tumor injection. This mixture, when given 1 wk in advance, produced a stronger antitumor effect by reducing the IL-17 and other angiogenesis factors. The difference in the immunomodulatory effects between the two modes of probiotic feeding may be explained by the recent findings using the Kaede-transgenic mice, which revealed a constant trafficking of immune cells between the intestine and other parts of the body (33). Early intake of probiotic may prepare the body with an antiinflammatory basis and limit the generation of excess Th17 cells in the gut that could be recruited to perpetuate protumor inflammation in other tissues. This notion is consistent with other observations where intake of antiinflammatory agents such as omega-3 polyunsaturated fatty acids is associated with reduced cancer risks (34). Interestingly, our metagenome analysis revealed the enhanced biogenesis of the DHA, one type of the omega-3 polyunsaturated fatty acids, confirming the antiinflammation effect in gut exerted by the probiotics.

Furthermore, we provided evidence that probiotics intake exhibited the potential of reducing the recruitment of Th17 from gut to tumor sites. Our observations are consistent with findings from a murine model of autoimmune diseases, such as experimental autoimmune encephalomyelitis and rheumatoid arthritis. In these studies, Th17 cells are homed from gut to distant inflammatory sites, such as the nervous system (35) and joints (36). The reduced Th17 level in the gut, by either modulating the gut microbiota with pathogens in germ-free animals or using antibiotics such as ampicillin, reduced the severity of these diseases (37). Th17 can express a number of chemokine receptors such as CCR6, CCR7, CXCR5, and CXCR6 to guide the migration of Th17 into the inflamed tissue (38). Th17 has been reported to migrate to tumors via the CCR6/CCL20 axis (39); consistent with these findings, we have found high levels of Th17 cells expressing CCR6 in control tumors, whereas this frequency has significantly reduced in the Prohep groups. Meanwhile, there is a reduced Th17 population in the gut of treatment groups, but not in other organs tested. This finding provided insight of regulating proinflammatory immune cell population in distant tumor sites via the crosstalk between gut and tumor.

Short-chain fatty acids (SCFAs) have been well documented for their antiinflammatory effects in the gut (40), and our study revealed the increased SCFAs-producer bacteria upon probiotics intake. Our pathway enrichment analysis shows that in the *ProPre* group the enriched Entner–Doudoroff pathway could lead to increased pyruvate, which would intensify acetyl-CoA production and increase the acetate conversion from acetyl-CoA via the enriched pathway of "acetate formation from acetyl-CoA I" (Fig. 4*C*). Subsequently, the enhanced transmission from pyruvate to acetate or propionate (Fig. 4 *B* and *C*) would increase the concentration of these two SCFAs in the gut. Thus, the entire synthetic route of SCFAs in the Prohep feeding groups was enhanced in the gut. Previous studies demonstrated that the SCFAs could down-regulate the proinflammatory cytokines, induce the differentiation of regulatory T cells, and suppress the Th17 polarization (41). Therefore, our metagenome sequencing provided strong evidence that probiotic intake would restructure the bacteria community composition from both taxonomy and functional perspective. The enriched organism or pathways are mainly related to the production of antiinflammatory compounds, including acetate, butyrate and propionate, or stimulate the differentiation of Treg or Tr1 cells. Apart from modulating the gut microbiota, we should not overlook the potential beneficial effect exerted directly from our probiotics. In vitro experiments showed that viable EcN and VSL#3 were potent inducers of IL-10 (11), whereas LGG stimulate IL-12 production from dendritic cells (42). These probiotics have shown potent effects in prevention and treatment of gut inflammation and IL-17–mediating autoimmune diseases (11). Nevertheless, we believe that the modulation of the gut microbiota by Prohep plays a more pivotal role because the quantity of bacteria cells and metabolites produced by the gut microbiota are much higher than the probiotic intake.

It is worth noting that the frequency of Th17 cells is significantly decreased, but IL-17 expression remains similar in the cisplatin group compared with the control. A previous in vitro study revealed that the TGF-β signaling pathway, which is required in differentiating Th17, would be deactivated when human testis cancer cell line was treated with cisplatin (43). In our study, TGF-β was down-regulated significantly in the cisplatin group (Fig. 2*A*). In addition, RORγt, the major transcriptional factor controlling the differentiation of Th17 was also down-regulated in the cisplatin group (Fig. 2*A*). The down-regulated TGF-β and RORγt suggested that the Th17 cells differentiation could be weakened in the tumor of the cisplatin group. At the same time, the reduction of migratory Th17 from intestine in the cisplatin group may also explain the reduced Th17 frequency in that group. Meanwhile, cisplatin is known to induce cancer stem cells or stem cell-like phenotype (44, 45). These cancer stem cells secrete large quantities of various proinflammatory mediators, including IL-17 (46), providing a possible explanation for the slightly increased (not significant) IL-17 in the cisplatin group. Nevertheless, we have not investigated the level of cancer stem cells, as this is beyond the scope of this study.

To better evaluate the beneficial effects of probiotics to HCC growth, we are planning to extend this study using an orthotopic model system, which provides a more realistic microenvironment encountered in the liver tumor. Further studies using metatranscriptome or metabolome analysis could help understand better the influence of probiotics on the gut metabolism and subsequently on other tissues beyond the intestinal tract.

Conclusions

In conclusion, a novel probiotic mixture named as Prohep was effective in reducing s.c. HCC growth significantly in mice. Th17 was likely to be the major producer of IL-17 in the tumor microenvironment that has linked to HCC growth and angiogenesis, and its decrease in tumor was probably related to the reduced recruitment from gut via circulation. The antitumor function

offered by Prohep was likely to associate with modulation of the gut microbiota by inducing the secretion of antiinflammatory IL-10 cytokine and suppressing Th17 cell differentiation in gut. The reduced recruited Th17 cells from gut and their secreted IL-17 weakened the angiogenesis in liver tumor and subsequently suppressed the tumor growth. We believe that our study has offered valuable insight into the molecular mechanism of the beneficially immunoregulatory effect of probiotics beyond gut level, which could be applied in prevention or treatment of cancer in extraintestinal sites.

Methods

Animals. Male C57BL6/N mice (5–6 wk old) were used in this study. Animals were allowed to acclimate for 1 wk before the conduction of experiments. In the s.c. tumor model, animals (n = 6–8) were fed ad libitum with probiotics or control (normal) diet starting from either 1 wk in advance or at the same day of tumor injection and killed at 38 d post-tumor injection or until humane end points were reached. All of the study protocols were approved by the Committee on the Use of Live Animals in Teaching and Research (CULATR) of the University of Hong Kong and the Department of Health of the Hong Kong Special Administrative Region (HKSAR) Government. All experiments on mice were performed in accordance with guidelines and regulations of University of Hong Kong and the Department of Health of the HKSAR Government. Please see *SI Methods* for more detailed descriptions.

Probiotics and Cisplatin. Prohep, a new probiotic mixture, is composed of *Lactobacillus rhamnosus* GG (LGG), viable *Escherichia coli* Nissle 1917 (EcN) and heat-inactivated VSL#3 (1:1:1). cis-Diamineplatinum (II) dichloride (Cisplatin; Sigma-Aldrich), a conventional anticancer agent that displays therapeutic efficacy in a broad range of solid tumors including liver cancer (47), was used as positive control. Please see *SI Methods* for more detailed descriptions.

Subcutaneous Tumor Model, IL-17 Antibody, and Cell Isolation. To induce tumor formation, Hepa1-6 (48) suspended in 100 μL of DMEM was injected s.c. using a 25-gauge needle. All tumor-bearing mice were killed at 38 d unless the humane endpoint was reached before that time.

To assess efficacy of probiotics on tumor growth, cisplatin was used as positive control. To evaluate the roles of IL-17+ cells in tumor progression, IL-17 neutralization was adopted by injecting 200 μg i.p. mouse anti–IL-17 (clone 17F3, BioXcell) 1 wk before tumor inoculation. Mice in control group were injected with isotype control antibody IgG (clone MOPC-21, BioXcell). The details about cell isolation can be found in the *SI Methods*.

RNA Extraction, cDNA Synthesis, and qRT-PCR. RNA was extracted with the TRIZOL Reagent (Life Technologies) following manufacturer's instructions. cDNA was synthesized from total RNA using the PrimeScript RT Master Mix reagent kit (Takara Bio) according to manufacturer's instructions. The quantitative real-time PCR (qRT-PCR) was evaluated using StepOnePlus Real-Time PCR System (Life Technologies). Please see *SI Methods* for more detailed descriptions.

Gut Metagenome Sequencing and Quality Control of the Raw Data. Mice stool were frozen at −80 °C immediately after collection. DNA extraction and library preparation followed the official protocols of the manufacturer (see *SI Methods* for more details). HiSeq 2000 was used for 100-bp paired-end (PE) sequencing with average yield of 6 Gb per sample. The raw sequences of eight samples can be found in NCBI Trace and Sequence Read Archive (SRA: SRP062583). The low quality reads or regions were filtered out using in-house script. Please see *SI Methods* for more detailed descriptions.

Taxonomy Profiling, Calculation of Community Diversity, and de Novo Assembly. We screened out all of the potential rRNA sequences using in-house pipeline (see *SI Methods* for the details) and deduced the taxonomy affiliation using RDP Classifier (49). The taxonomic alpha diversity, taxonomic and functional beta diversity were calculated by in-house scripts and some R packages (see *SI Methods* for the details). IDBA-UD (50) was adopted to achieve the de novo assembly with the k-mer size ranging from 20 to 100 bp. Please see *SI Methods* for gene prediction, function, and pathway annotation.

Statistical Tests. All of the statistical tests in experimental parts, including tumor size, qPCR, and cell frequency, etc., were performed using t test between each treatment group and control group. To detect the significantly varied pathways, the median difference of abundance (RPKM) before and during treatment for the genes in the same EC category was tested using the Wilcoxon signed-rank test (51).

ACKNOWLEDGMENTS. J.L. and G.P. thank the Strategic Research Themes (SRT) of Genomics of The University of Hong Kong (HKU) for their support and the emerging Strategic Research Themes of Integrative Biology (HKU) for fruitful discussions. This project was supported by HKU Small Grant Funding 201409176144.

1. IARC (2013) *GLOBOCAN 2012: Estimated Cancer Incidence, Mortality and Prevalence Worldwide in 2012* (International Agency for Research on Cancer, Lyon, France).
2. Fernández M, et al. (2009) Angiogenesis in liver disease. *J Hepatol* 50(3):604–620.
3. Ono M (2008) Molecular links between tumor angiogenesis and inflammation: Inflammatory stimuli of macrophages and cancer cells as targets for therapeutic strategy. *Cancer Sci* 99(8):1501–1506.
4. Cua DJ, Tato CM (2010) Innate IL-17-producing cells: The sentinels of the immune system. *Nat Rev Immunol* 10(7):479–489.
5. Murugaiyan G, Saha B (2009) Protumor vs antitumor functions of IL-17. *J Immunol* 183(7):4169–4175.
6. Numasaki M, et al. (2003) Interleukin-17 promotes angiogenesis and tumor growth. *Blood* 101(7):2620–2627.
7. Chauhan SK, et al. (2011) A novel pro-lymphangiogenic function for Th17/IL-17. *Blood* 118(17):4630–4634.
8. Numasaki M, et al. (2005) IL-17 enhances the net angiogenic activity and in vivo growth of human non-small cell lung cancer in SCID mice through promoting CXCR-2-dependent angiogenesis. *J Immunol* 175(9):6177–6189.
9. Lee JW, et al. (2008) Differential regulation of chemokines by IL-17 in colonic epithelial cells. *J Immunol* 181(9):6536–6545.
10. Ivanov II, et al. (2008) Specific microbiota direct the differentiation of IL-17-producing T-helper cells in the mucosa of the small intestine. *Cell Host Microbe* 4(4):337–349.
11. Tanabe S (2013) The effect of probiotics and gut microbiota on Th17 cells. *Int Rev Immunol* 32(5-6):511–525.
12. Plottel CS, Blaser MJ (2011) Microbiome and malignancy. *Cell Host Microbe* 10(4):324–335.
13. Berger H, et al. (2013) SOCS3 transactivation by PPARγ prevents IL-17-driven cancer growth. *Cancer Res* 73(12):3578–3590.
14. Augustin R (2010) The protein family of glucose transport facilitators: It's not only about glucose after all. *IUBMB Life* 62(5):315–333.
15. Bogaerts E, et al. (2015) Time-dependent effect of hypoxia on tumor progression and liver progenitor cell markers in primary liver tumors. *PLoS One* 10(3):e0119555.
16. Amann T, et al. (2009) GLUT1 expression is increased in hepatocellular carcinoma and promotes tumorigenesis. *Am J Pathol* 174(4):1544–1552.
17. Denko NC (2008) Hypoxia, HIF1 and glucose metabolism in the solid tumour. *Nat Rev Cancer* 8(9):705–713.
18. Guinane CM, Cotter PD (2013) Role of the gut microbiota in health and chronic gastrointestinal disease: Understanding a hidden metabolic organ. *Therap Adv Gastroenterol* 6(4):295–308.
19. Holmes E, Li JV, Marchesi JR, Nicholson JK (2012) Gut microbiota composition and activity in relation to host metabolic phenotype and disease risk. *Cell Metab* 16(5):559–564.
20. Maslowski KM, Mackay CR (2011) Diet, gut microbiota and immune responses. *Nat Immunol* 12(1):5–9.
21. Ahn J, et al. (2013) Human gut microbiome and risk for colorectal cancer. *J Natl Cancer Inst* 105(24):1907–1911.
22. Scanlan PD, et al. (2008) Culture-independent analysis of the gut microbiota in colorectal cancer and polyposis. *Environ Microbiol* 10(3):789–798.
23. Amato KR, et al. (2013) Habitat degradation impacts black howler monkey (Alouatta pigra) gastrointestinal microbiomes. *ISME J* 7(7):1344–1353.
24. Schwiertz A, et al. (2010) Microbiota and SCFA in lean and overweight healthy subjects. *Obesity (Silver Spring)* 18(1):190–195.
25. Brown CT, et al. (2011) Gut microbiome metagenomics analysis suggests a functional model for the development of autoimmunity for type 1 diabetes. *PLoS One* 6(10):e25792.
26. Kverka M, et al. (2011) Oral administration of Parabacteroides distasonis antigens attenuates experimental murine colitis through modulation of immunity and microbiota composition. *Clin Exp Immunol* 163(2):250–259.
27. Arpaia N, et al. (2013) Metabolites produced by commensal bacteria promote peripheral regulatory T-cell generation. *Nature* 504(7480):451–455.
28. Round JL, Mazmanian SK (2010) Inducible Foxp3+ regulatory T-cell development by a commensal bacterium of the intestinal microbiota. *Proc Natl Acad Sci USA* 107(27):12204–12209.
29. Iida N, et al. (2013) Commensal bacteria control cancer response to therapy by modulating the tumor microenvironment. *Science* 342(6161):967–970.
30. Yang ZH, Miyahara H, Hatanaka A (2011) Chronic administration of palmitoleic acid reduces insulin resistance and hepatic lipid accumulation in KK-Ay Mice with genetic type 2 diabetes. *Lipids Health Dis* 10:120.
31. De Caterina R, Cybulsky MI, Clinton SK, Gimbrone MA, Jr, Libby P (1994) The omega-3 fatty acid docosahexaenoate reduces cytokine-induced expression of proatherogenic and proinflammatory proteins in human endothelial cells. *Arterioscler Thromb* 14(11):1829–1836.

32. Llovet JM, et al.; SHARP Investigators Study Group (2008) Sorafenib in advanced hepatocellular carcinoma. *N Engl J Med* 359(4):378–390.
33. Ding Y, Xu J, Bromberg JS (2012) Regulatory T cell migration during an immune response. *Trends Immunol* 33(4):174–180.
34. Murff HJ, et al. (2011) Dietary polyunsaturated fatty acids and breast cancer risk in Chinese women: A prospective cohort study. *Int J Cancer* 128(6):1434–1441.
35. Arima Y, et al. (2012) Regional neural activation defines a gateway for autoreactive T cells to cross the blood-brain barrier. *Cell* 148(3):447–457.
36. Murakami M, et al. (2011) Local microbleeding facilitates IL-6- and IL-17-dependent arthritis in the absence of tissue antigen recognition by activated T cells. *J Exp Med* 208(1):103–114.
37. Bedoya SK, Lam B, Lau K, Larkin J, 3rd (2013) Th17 cells in immunity and autoimmunity. *Clin Dev Immunol* 2013:986789.
38. Kim CH (2009) Migration and function of Th17 cells. *Inflamm Allergy Drug Targets* 8(3):221–228.
39. Zou W, Restifo NP (2010) T(H)17 cells in tumour immunity and immunotherapy. *Nat Rev Immunol* 10(4):248–256.
40. Lomax AR, Calder PC (2009) Probiotics, immune function, infection and inflammation: A review of the evidence from studies conducted in humans. *Curr Pharm Des* 15(13): 1428–1518.
41. Smith PM, et al. (2013) The microbial metabolites, short-chain fatty acids, regulate colonic Treg cell homeostasis. *Science* 341(6145):569–573.
42. Kim JY, Park MS, Ji GE (2012) Probiotic modulation of dendritic cells co-cultured with intestinal epithelial cells. *World J Gastroenterol* 18(12):1308–1318.
43. Duale N, et al. (2007) Molecular portrait of cisplatin induced response in human testis cancer cell lines based on gene expression profiles. *Mol Cancer* 6:53.
44. Rosanò L, et al. (2011) Acquisition of chemoresistance and EMT phenotype is linked with activation of the endothelin A receptor pathway in ovarian carcinoma cells. *Clin Cancer Res* 17(8):2350–2360.
45. Nör C, et al. (2014) Cisplatin induces Bmi-1 and enhances the stem cell fraction in head and neck cancer. *Neoplasia* 16(2):137–146.
46. Sun Z, Wang S, Zhao RC (2014) The roles of mesenchymal stem cells in tumor inflammatory microenvironment. *J Hematol Oncol* 7:14.
47. Carr BI (2002) Hepatic artery chemoembolization for advanced stage HCC: Experience of 650 patients. *Hepatogastroenterology* 49(43):79–86.
48. Kröger A, et al. (2001) Growth suppression of the hepatocellular carcinoma cell line Hepa1-6 by an activatable interferon regulatory factor-1 in mice. *Cancer Res* 61(6): 2609–2617.
49. Wang Q, Garrity GM, Tiedje JM, Cole JR (2007) Naive Bayesian classifier for rapid assignment of rRNA sequences into the new bacterial taxonomy. *Appl Environ Microbiol* 73(16):5261–5267.
50. Peng Y, Leung HC, Yiu SM, Chin FY (2012) IDBA-UD: A de novo assembler for single-cell and metagenomic sequencing data with highly uneven depth. *Bioinformatics* 28(11):1420–1428.
51. Wilcoxon F (1945) Individual comparisons by ranking methods. *Biom Bull* 1(6):80–83.
52. Kruis W, et al. (2004) Maintaining remission of ulcerative colitis with the probiotic Escherichia coli Nissle 1917 is as effective as with standard mesalazine. *Gut* 53(11): 1617–1623.
53. Fedorak RN, et al. (2003) VSL3 probiotic mixture induces remission in patients with active ulcerative colitis. *Gastroenterology* 124(4):A377.
54. Gupta P, Andrew H, Kirschner BS, Guandalini S (2000) Is lactobacillus GG helpful in children with Crohn's disease? Results of a preliminary, open-label study. *J Pediatr Gastroenterol Nutr* 31(4):453–457.
55. Li H, Durbin R (2009) Fast and accurate short read alignment with Burrows-Wheeler transform. *Bioinformatics* 25(14):1754–1760.
56. Altschul SF, Gish W, Miller W, Myers EW, Lipman DJ (1990) Basic local alignment search tool. *J Mol Biol* 215(3):403–410.
57. Quast C, et al. (2013) The SILVA ribosomal RNA gene database project: Improved data processing and web-based tools. *Nucleic Acids Res* 41(Database issue): D590–D596.
58. McMurdie PJ, Holmes S (2013) phyloseq: An R package for reproducible interactive analysis and graphics of microbiome census data. *PLoS One* 8(4):e61217.
59. Wood DE, Salzberg SL (2014) Kraken: Ultrafast metagenomic sequence classification using exact alignments. *Genome Biol* 15(3):R46.
60. Dixon P (2009) VEGAN, a package of R functions for community ecology. *Journal of Vegetation Science* 14(6):927–930.
61. Zhu W, Lomsadze A, Borodovsky M (2010) Ab initio gene identification in metagenomic sequences. *Nucleic Acids Res* 38(12):e132.
62. Tatusov RL, Koonin EV, Lipman DJ (1997) A genomic perspective on protein families. *Science* 278(5338):631–637.
63. Claudel-Renard C, Chevalet C, Faraut T, Kahn D (2003) Enzyme-specific profiles for genome annotation: PRIAM. *Nucleic Acids Res* 31(22):6633–6639.
64. Ye Y, Doak TG (2009) A parsimony approach to biological pathway reconstruction/inference for genomes and metagenomes. *PLOS Comput Biol* 5(8):e1000465.